European Polymer Journal 214 (2024) 113150

Contents lists available at ScienceDirect

European Polymer Journal

journal homepage: www.elsevier.com/locate/europolj

Introducing Targeting Units or pH-Releasable Immunodrugs into Core-Clickable Nanogels

Alina G. Heck [a], David Schwiertz [b], Bellinda Lantzberg [a], Ha-Chi Nguyen [a], Robert Forster [c], Maximilian Scherger [a], Till Opatz [c], Jo A. Van Ginderachter [d,e], Lutz Nuhn [a,f,*]

[a] Max Planck Institute for Polymer Research, 55128 Mainz, Germany
[b] Biotherapeutics Division, Leiden Academic Centre for Drug Research (LACDR), Leiden University, 2333CC Leiden, the Netherlands
[c] Johannes Gutenberg-University Mainz, Department of Chemistry, 55128 Mainz, Germany
[d] Brussels Center for Immunology, Vrije Universiteit Brussel, 1050 Brussels, Belgium
[e] Myeloid Cell Immunology Lab, VIB Center for Inflammation Research, 1050 Brussels, Belgium
[f] Chair of Macromolecular Chemistry, Julius-Maximilians-Universität Würzburg, 97070 Würzburg, Germany

ARTICLE INFO

Keywords:
DBCO click chemistry
RAFT-polymerization
Mannose targeting
2-propionic-3-methylmaleic anhydride linker
DBCO nanogels
pH-reversible drug-loaded nanogels
Immunodrug delivery

ABSTRACT

The development of nano-sized carrier systems plays a fundamental role in immunodrug delivery and the treatment of cancer. Especially functional materials, coupled with a stimuli-responsive drug release, control the selective delivery of small molecular drugs to the target site and avoid systemic side effects. Based on this, we introduce a DBCO core-functionalized nanogel platform for pH-reversible conjugation of highly potent TLR7/8-activating imidazoquinolines and the selective targeting of macrophage mannose receptor (MMR/ CD206) expressed by immunosuppressive macrophages. DBCO-PEG_4-amine functionalized polymethacrylates are synthesized by controlled RAFT polymerization and self-assembled into precursor micelles in polar aprotic solvents. Corresponding nanogels are generated *via* reactive ester chemistry, while conjugated DBCO–units are incorporated into the core, still accessible for click reaction with azide-functionalized structures. Regarding the preparation of targeted nanogels, trimannose equipped with azide moieties can be conjugated to the DBCO nanogels, revealing the efficient targeting of macrophages' mannose receptor *in vitro*. Moreover, the broad applicability of the DBCO nanogel is demonstrated by the synthesis of an azide–containing 2-propionic-3-methylmaleic anhydride-based linker sensitive for the pH–reversible conjugation of secondary amine-modified immune modulators, such as IMDQ-Me. *Via* bioorthogonal DBCO click reaction, the immune modulator can reversibly be conjugated, affording pH-responsive drug-loaded nanogels that conserve the desired immune stimulatory effect *in vitro*. Overall, these findings highlight the potential of core–functionalized DBCO nanogels, a promising carrier system for pH–sensitive conjugated immunodrugs as well as an attractive platform for controlled targeting of MMR. Altogether, the versatile application of core-functionalized DBCO nanogels may pave the way for enhancing bioorthogonal multifunctionality inside nanocarrier systems that assist in addressing multiple targets in cancer immunotherapy.

1. Introduction

Nano-scaled polymeric micelles have demonstrated a high potential as drug delivery system in diagnostics and therapeutics. The variation of the pharmacokinetic profile, as well as the improved bioavailability and reduced toxicity of small-molecular drugs increased the application of nanoparticles in anticancer therapy. Thus far, efficient targeted drug delivery has primarily been accomplished by the accumulation of long circulating drug nanoformulations using the enhanced permeability and retention (EPR) effect of solid tumors [1–4]. Based on the high demand for nutrients and oxygen, fast growing tumors present various leaky vessels which increases the permeability to nanomaterials, while contributing to the retention time through the lack of normal lymphatic drainage [5,6]. Compared to passive targeting, active targeting relies on the application of targeting structures conjugated to nanoparticles. Accumulated in the tumor microenvironment, biological ligands can

* Corresponding author at: Julius-Maximilians-Universität Würzburg, 97070 Würzburg, Germany, Max Planck Institute for Polymer Research, 55128 Mainz, Germany.
E-mail addresses: lutz.nuhn@uni-wuerzburg.de, lutz.nuhn@mpip-mainz.mpg.de (L. Nuhn).

https://doi.org/10.1016/j.eurpolymj.2024.113150
Received 29 February 2024; Received in revised form 12 May 2024; Accepted 17 May 2024
Available online 19 May 2024

interact with specific receptors or markers overexpressed on tumor or immune cells affording a cell-specific drug delivery [6,7]. Already illustrated by the Ringsdorf model for pharmacologically active polymers [8,9] targeted carrier structures improve the efficacy at the site of the disease. Small structures like nanobodies [10,11] or saccharides [12] are promising mediators for a cell-selective drug targeting. Mannose receptors are expressed on important immune cells, including dendritic cells and macrophages [12,13]. Among these cells, macrophages are represented in all tissues, while playing a dominant role in tumor progression and metastasis. Tumor-associated macrophages (TAMs) are located in the tumor microenvironment, often displaying a high immunosuppressive activity and strong expression of the Macrophage Mannose Receptor (MMR, CD206). Hence, TAMs can be considered as an attractive target for cancer immunotherapy [11,14–17].

Access to nano-sized drug delivery systems can be generated by the synthesis of self–assembling block copolymers [1,18]. Subsequent core-crosslinking will then assist in providing advanced properties for applications in complex biological environments [4,19,20]. As already reported from our laboratories, well-defined core–shell systems can be formulated by the Reversible Addition-Fragmentation Chain Transfer (RAFT) polymerization of methoxy tri(ethylene glycol) methacrylate (mTEGMA) and the reactive ester pentafluorophenyl methacrylate (PFPMA) [21]. The resulting amphiphilic block copolymers provide efficient shielding properties and stability based on the hydrophilic PEG-like structure, whereas the hydrophobic PFPMA enables controlled self-assembly and amine modification [22–24]. Consequently, self-assembled micelles can be further functionalized by dye-labeling or core–crosslinking, promoting the nanoparticle stability and integrity [22,25]. So far, additional surface decoration with azides enabled the conjugation of DBCO-functional proteins or peptides and the generation of antigen-decorated nanogels [25,26]. Additionally, MMR-targeting nanobodies were also immobilized onto such nanogels for targeting $CD206^+$ cells [10,14]. However, the core-functionalization with amine–containing dibenzocyclooctynes (DBCO) has not been reported yet and could further extend the application of our nanoparticle system. To that respect, latest investigations from our group conclude that for similar core-crosslinked nanogels which switch their core polarity from hydrophobic to hydrophilic consequently provide a more porous structure where not only water but also other guest molecules can diffuse into the core [53]. The DBCO group would then permanently immobilize azide-functionalized guest molecules *via* click chemistry.

In recent years, click chemistry has become an important tool in nanomedicine and pharmaceutical sciences. Since the first reports by Sharpless and coworkers in 2001, click chemistry has been defined as high-yielding reactions, providing non-reacting by-products under mild reaction conditions [27,28]. Various bioorthogonal reactions such as the copper-catalyzed azide-alkyne cycloaddition (CuAAC) or the tetrazine ligation by an inverse electron-demand Diels-Alder reaction (IEDDA) have paved the way for a fast and selective chemical reaction between biomolecules and synthesized functional groups. Due to the general concern of copper in materials for biomedical applications, the Cu-free azide-alkyne cycloaddition (SPAAC) demonstrates efficient reaction properties with milder and more versatile application features. Strained cyclooctynes such as DBCO form chemically and metabolically robust bonds to orthogonal azides in a [2+3] cycloaddition, making the reaction an attractive candidate for numerous *in situ* applications [29–31].

Hence, SPAAC reactions can be used to modify nanocarriers with additional functional groups or stimuli responsive systems. Supplementation of nano-sized drug carriers with stimuli responsive motives promotes a controlled drug efficacy at the target-site with minimized side effects. Among the variety of stimuli such as light or redox potential, pH-sensitive formulations gained an important role in next generation nanomaterials [32–34]. Between frequently used ketal [24] or hydrazone structures, [35] disubstituted maleic anhydride systems have been employed as excellent structures able to release conjugated amines in their native form without the generation of by-products [36,37]. Already a mildly acidic pH (5.5–6.8) initiates the fast attack by the β–positioned free carboxylic acid to the amide, resulting in the reformation of the anhydride system and precursor amines [34,38,39]. In addition, modification of the *cis*-double bond by variation of adjacent substituents impacts the angle between maleic acid amide derivates and the β-carboxylate and, thus, the pH sensitivity of the system [40–42]. When primary amines are conjugated, we recently reported the formation of cyclic imides on polymeric maleic anhydrides resulting in the lack of pH sensitivity [43]. Only for secondary amines, reversibility of the conjugate is found. Consequently, we could support the pH-reversible conjugation of secondary amine-containing drugs, such as the small-molecular Toll-like receptor 7/8 (TLR7/8) agonist 1-(4-((methylamino)methyl)-benzyl)-2-butyl-1*H*-imidazo[4,5-c]quinolin-4-amine (IMDQ-Me) [43].

Upon administration most TLR agonists activate various antigen-presenting cells (APCs) leading to the secretion of cytokines like type-I IFN and IL-12 and the stimulation of cytotoxic T–cells. Nevertheless, most injected compounds rapidly distribute through the body, resulting in an undesired inflammatory reaction [23,24,44,45]. Previous reports demonstrated a controlled immune activation by covalent conjugation of small molecular TLR agonists to different types of nanocarriers [25,46–48]. In this context, the additional application of stimuli-responsive linkers could contribute to the efficacy and targeted immune stimulation.

Herein, we describe the conjugation of an amine-functionalized DBCO to an amphiphilic block copolymer consisting of methoxy tri (ethylene glycol) methacrylate (mTEGMA) and reactive ester pentafluorophenyl methacrylate (PFPMA), followed by the conversion of the block copolymer micelles into completely hydrophilic dye-labeled and core-crosslinked nanogels (Fig. 1). Investigating the accessibility of the nanogels' core-localized DBCO groups with azide-containing dyes, the favourable click reaction is shown and paving the way for biological applications. While the nanogel itself shows no MMR affinity, covalent conjugation of an azide-functionalized trimannose triggers the selective targeting and internalization into MMR-expressing cells. Further generation of an azide-modified disubstituted maleic anhydride linker offers a smart platform for the pH–sensitive conjugation of different amines as well as secondary amine-modified immune-stimulating TLR 7/8 agonist IMDQ-Me with high *in vitro* activity. Overall, extending the nanogel platform for DBCO click reactions therefore provides beneficial features for a targeted and pH-sensitive (immuno)-drug delivery.

2. Results and discussion

2.1. Design, synthesis and characterization of a DBCO-functionalized nanogel platform

To establish a synthetic pathway for DBCO-conjugated amphiphilic block copolymers, pentafluorophenyl (PFP) reactive ester monomers were employed [49,50]. With their high solubility in different organic solvents, their high reactivity for a broad range of amines and their easy direction of reaction kinetics, [51,52] pentafluorophenyl methacrylate (PFPMA) monomers were accessed by treatment of methacryloyl chloride with pentafluorophenol (Figure S1-S4). Next, Reversible Addition-Fragmentation Chain Transfer (RAFT) polymerisation should enable the controlled synthesis of the block copolymer $p(mTEGMA)_n$–*b*–$p(PFPMA)_m$ to form block copolymer micelles, followed by the conversion into hydrophilic nanogels. Therefore, commercially available tri (ethylene glycol)methyl ether methacrylate (mTEGMA) was polymerized by the chain transfer agent 4–cyano-4-((phenylcarbonothioyl)thio) pentanoic acid and the initiator azobisisobutyronitrile (AIBN, Figure S5). Precipitation in hexane yielded the homopolymer $p(mTEGMA)_{20}$ with an apparent number-average molecular weight ($M_{n,app}$) of 2700 g/mol and a narrow $Đ$ of 1.22 (Figure S6 + S7 – SEC in THF with PMMA calibration). Afterwards, similar reaction conditions were applied during block copolymerization with PFPMA (Figure S8) yielding

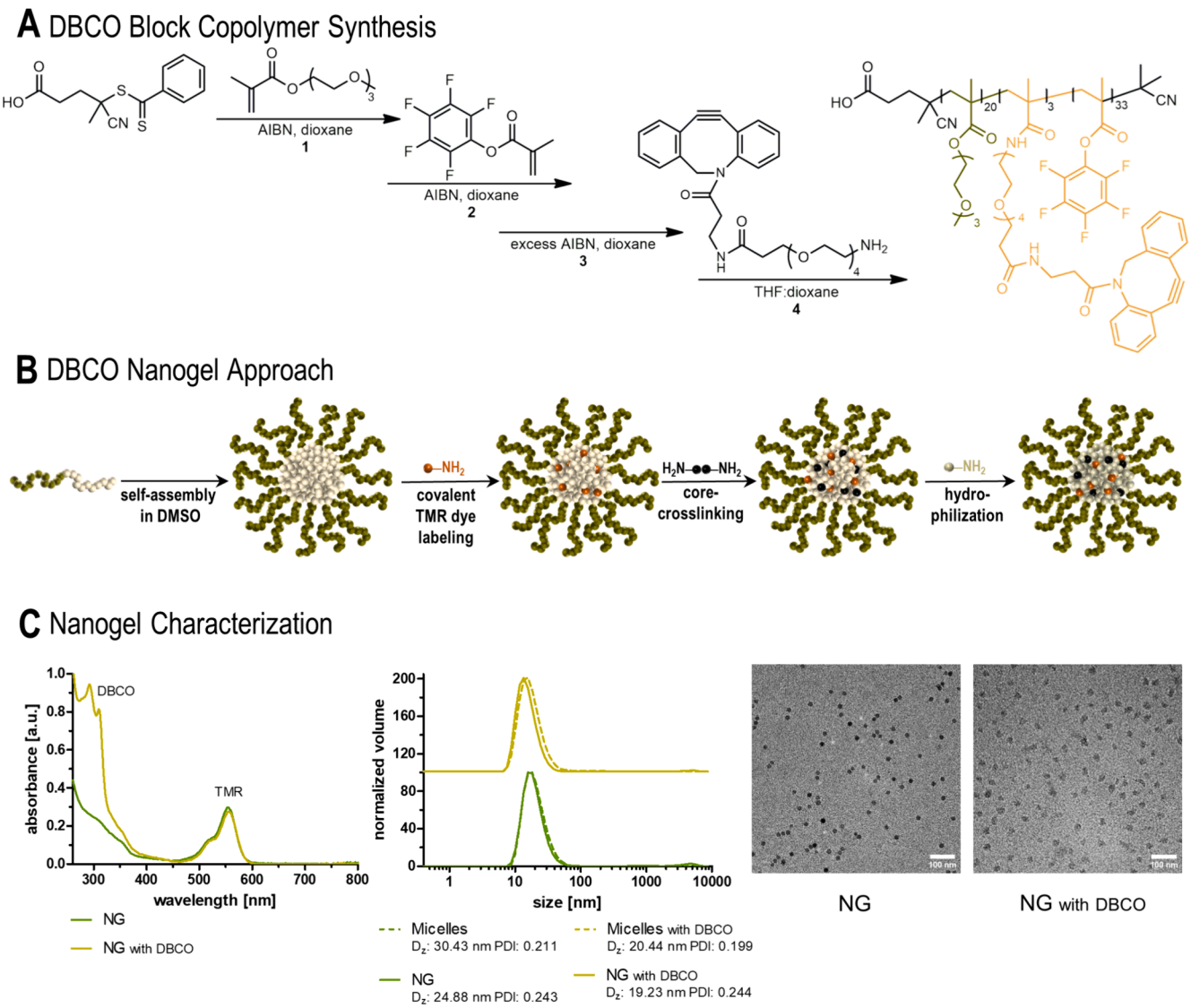

Fig. 1. Preparation of core-functionalized DBCO nanogels from DBCO-containing reactive ester block copolymer. (A) Synthesis scheme for the controlled RAFT block copolymerization of p(mTEGMA) with PFPMA initiated by AIBN affording the block copolymer p(mTEGMA)$_{20}$-*b*-p(PFPMA)$_{36}$, followed by partial modification through aminolysis with DBCO-PEG$_4$-amine. (B) Sequential fabrication process for the core-localized DBCO nanogels derived from the self-assembled precursor micelles in DMSO. The remaining reactive ester chemistry units enable the generation of tetramethylrhodamine dye (TMR)-labeled and core-crosslinked, hydrophilic nanogels. (C) Characterization data for the DBCO nanogels compared to nanogels without DBCO. In the UV-spectra of both TMR-labeled nanogels, the absorbance maxima around 300 nm can be related to the nanogel core-conjugated DBCO units. Dynamic light scattering (DLS) measurements of the precursor micelles and fabricated nanogels both with and without DBCO-conjugated. Subsequent transmission electron microscopy (TEM) images confirm the homogeneity of both nanogels with and without DBCO.

a narrowly dispersed block copolymer with a $Đ$ of 1.28 and apparent number-average molecular weight ($M_{n,app}$) of 10600 g/mol. Thereby, a significant shift of the block copolymer by size exclusion chromatography (SEC) compared to the homopolymer clearly attested the attachment of PFPMA to the homopolymer (Figure S11). Further ^{1}H NMR and ^{19}F NMR spectroscopy characterization (Figure S9 and S10) confirmed the successful synthesis of the block copolymer p(mTEGMA)$_{20}$-*b*-p(PFPMA)$_{36}$. To ensure no interaction of the dithiobenzoate end groups with amines present during the nanogel formulation, the block copolymer was further reacted with an excess of AIBN (Figure S13). Here, the removal of the end groups was confirmed by UV–Vis spectroscopy but had no effect on the structural properties of the block copolymer (Figure S13-S15).

In a final step, the block copolymer was partially functionalized with DBCO through aminolysis by DBCO-PEG$_4$–amine (Fig. 1A and Figure S16). The modified block copolymer chains were targeted to be equipped with three DBCO-PEG$_4$-units per chain and could then be isolated by precipitation in diethyl ether. Detailed characterization was conducted by ^{1}H, ^{19}F NMR and UV–Vis spectroscopy, as well as size exclusion chromatography (SEC, Figure S17-S19) which all confirmed the covalent conjugation of the DBCO group onto the p(PFPMA) block.

For the preparation of fully hydrophilic nanogels, precursor micelles were prepared from p(mTEGMA)$_{20}$-*b*-p(PFPMA)$_{36}$ with or without additional DBCO modification. Both block copolymers could be self-assembled in DMSO by ultrasonication. As demonstrated in our earlier work, [14,19–25,54–57,64–66] the fluorophilic nature of the p(PFPMA)-block causes a phase separation in polar aprotic solvents affording block copolymer micelles that could be detected for the p(mTEGMA)$_{20}$-*b*-p(PFPMA)$_{36}$ block copolymers with or without DBCO by dynamic light scattering (DLS) in DMSO. The two systems provided narrowly distributed micelles with a z-average hydrodynamic diameter (D_z) between 20 to 30 nm and a PDI of 0.20. Interestingly, the DBCO

micelles tended to be slightly smaller, considering their lower degree of fluorination which governs the polymers' self-assembly in DMSO (Fig. 1C and Figure S19). Following the synthesis concept of Fig. 1B (and Figure S20), the remaining PFP units were subsequently aminolyzed by traces of tetramethylrhodamine cadaverine (TMR) for dye labeling and 0.5 equivalents of 2,2-(ethylenedioxy)bis(ethylamine) for cross-linking. Final hydrophilization by an excess of 2–aminoethanol, followed by purification *via* dialysis against millipore water supplemented with 0.1 % ammonia resulted in two types of nanogels (NG and NG with DBCO). To ensure the integrity of the nanogels and their core-localized DBCO units, UV–Vis absorbance spectra and DLS measurement were recorded in millipore water containing 0.1 % ammonia (Fig. 1C and Figure S21). Thereby, both systems revealed the successful generation of TMR–labeled nanogels with narrow monomodal distribution in a similar size range (D_z of 19.23 nm and 24.88 nm – the DBCO functionality does obviously not interfere with the nanogel later on, as the particle sizes were pre-determined by self-assembled smaller precursor micelles). In addition, the core-crosslinked nanogels could be imaged in dry state by transmission electron microscopy (TEM) and confirmed the presence of homogenously distributed spherically shaped nanoparticles. Interestingly, DBCO–functionalized nanoparticles illustrated a spherical morphology with slightly reduced contrast (Fig. 1C – perhaps the loss of fluorine content may slightly disturb the intramicellar nanophase separation of the precursor micelles).

With respect to the further preparation of drug-loaded or targeted nanogels, the accessibility of the nanogels' DBCO-units during bioorthogonal conjugation had to be confirmed. Consequently, a commercially available azide-modified fluorescent dye (Oregon Green 488 azide, OG488 azide) was used for tracing its click attachment to the nanogel, while potentially unreacted dyes could be removed *via* spin-filtrations, particularly important for control nanogels that do not contain any DBCO-groups. The isolated nanogels were analyzed by UV–Vis and DLS measurement, showing an additional absorbance maximum at 496 nm only for the DBCO nanogels (Fig. 2B and 2C). In contrast, OG488 azide-treated control nanogels (NG) revealed only one absorbance maximum at 550 nm, derived from the conjugated TMR. In conclusion, the nanogels' DBCO-groups can be addressed for click chemistry and represent an ideal candidate for selective drug delivery by post-modification inside the nanogels' cores. This observation matches well with our recent observations on similar micelle-derived core-crosslinked and hydrophilized nanogels. They seem to provide a more porous structure and allow not only water to enter the nanoparticle but also other guest molecules to diffuse into the nanogel core [53].

2.2. *Modification of DBCO nanogels with Azide-Trimannose for controlled MMR targeting*

Glycosylation can confer excellent targeting properties and consequently aid in understanding of a variety of cellular recognition processes. Due to its high specificity and effectiveness, mannosylation can be used for selective targeting of immune cells that highly express the mannose receptor, such as macrophages or dendritic cells, paving the way towards improved drug delivery and controlled immunotherapy [13,14,16,54–57]. Therefore, we aimed at conjugating azide-containing trimannose motifs [58,59] to the DBCO-functionalized nanogels (Fig. 3A and Figure S38).

For comprehensive confirmation of successful trimannose conjugation, the nanogels were further treated with an azide-functionalized fluorescent dye (AF488 azide) after the azide trimannose modification (Fig. 3A). If successful trimannose conjugation occurred first, the dye can afterwards not conjugate compared to previous experiments. Additional control reactions on nanogels without DBCO should serve as further proof for selective trimannose nanogel formation (Figure S38). Following the reaction scheme of Fig. 3A (and Figure S38), all nanogels were subsequently purified by excessive spin-filtration for removal of unconjugated compounds, and then characterized by DLS and UV-measurement. Trimannose conjugation or dye-labeling did not affect the size of the nanogels (Fig. 3B).

Furthermore, DBCO nanogels solely treated with AF488 azide demonstrated a significant absorbance maximum at 496 nm (Fig. 3C). In stark contrast, DBCO nanogels which first reacted with azide trimannose led to the conversion of all potential DBCO–groups, and consequently no AF488 dye could be bound but was removed during the purification step. In case of control nanogel reactions without DBCO, a conjugation

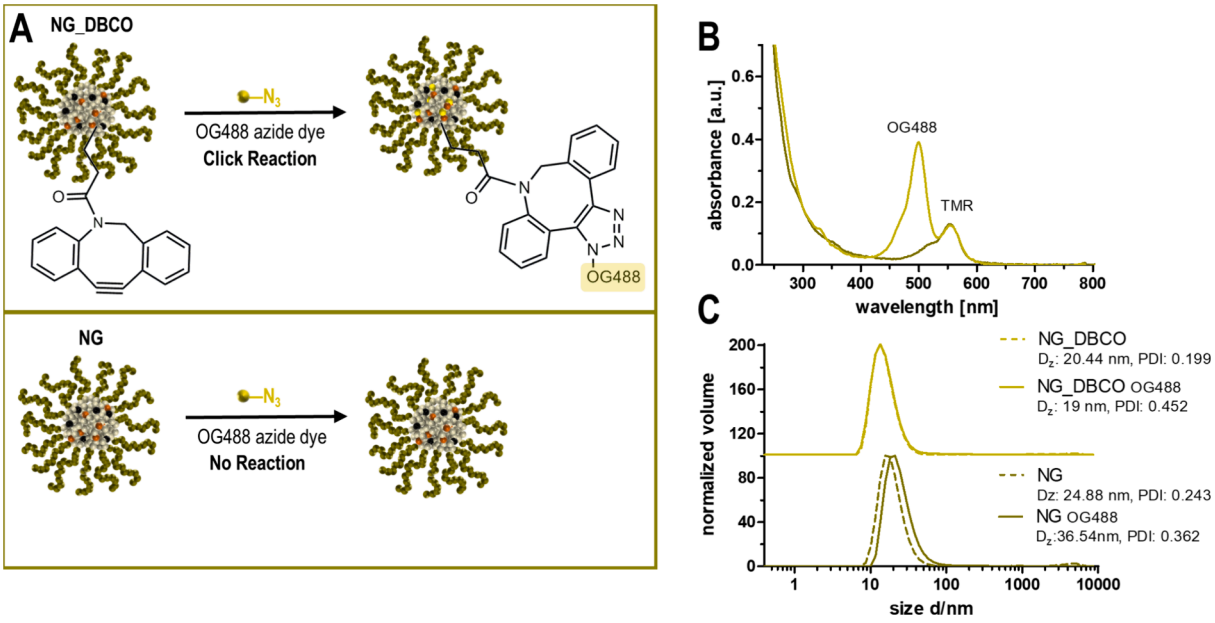

Fig. 2. Analyzing the accessibility of the nanogels' core-localized DBCO-units. (A) Schematic reaction of the DBCO nanogel with the azide-containing fluorescent dye Oregon Green 488 azide (OG488 azide) compared to nanogels without core-localized DBCO. (B) UV–Vis spectra of the dye-functionalized DBCO nanogels, revealing an additional absorbance maximum at 496 nm only for the DBCO nanogels while the control nanogels show no reaction with OG488 azide. (C) DLS measurements of the DBCO nanogels and control nanogels before and after treatment with OG488 azide. (For interpretation of the references to colour in this figure legend, the reader is referred to the web version of this article.)

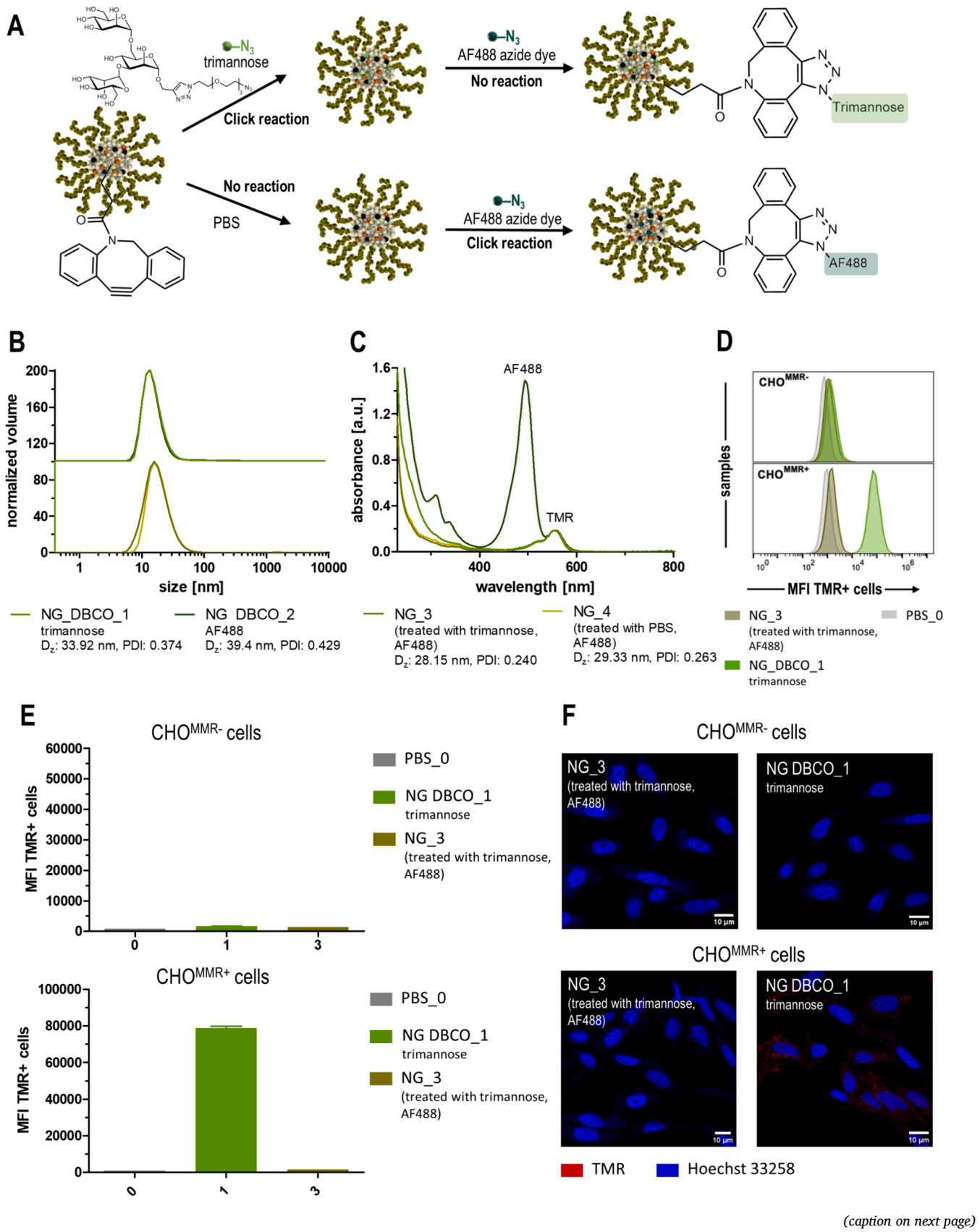

(caption on next page)

Fig. 3. Formulation of trimannose conjugated DBCO nanogels for specific targeting of the macrophage mannose receptor (MMR) *in vitro*. (A) Reaction scheme for the sequential attachment of trimannose and Alexa Fluor 488 azide (AF488 azide) to the DBCO nanogel core by click reaction. (B) DLS measurement of the trimannose (NG_DBCO_1) and AF488-labeled (NG_DBCO_2) nanogels as well as corresponding control nanogels without DBCO (NG_3 and NG_4), which were treated accordingly to the DBCO nanogels but cannot undergo any conjugation. (C) UV–Vis spectrophotometry data of the nanoparticles shows an additional absorbance maximum at 488 nm only for NG_DBCO_2 solely treated with AF488 azide, while NG_DBCO_1 has previously been reacted with trimannose and, thus, shows no additional absorbance maximum. It can consequently be assumed to be successfully conjugated to trimannose. (D) Cellular histogram of $CHO^{MMR+/MMR-}$ cells incubated with trimannose-labeled DBCO nanogels and PBS as a reference at 10 μg/mL for 24 h (n = 3). (E) Mean fluorescence intensities (MFI) of $CHO^{MMR+/MMR-}$ cells incubated with TMR-labeled nanogels which were treated with trimannose and then AF448 azide (DBCO_NG_1 or NG_3) at 10 μg/mL for 24 h (n = 3). Only the DBCO_NG_1, accessible for trimannose click reaction, demonstrated a specific uptake in CHO^{MMR+} cells. (F) Confocal microscopy images of $CHO^{MMR+/MMR-}$ cells incubated with DBCO_NG_1 or NG_3 at 10 μg/mL for 24 h (red: TMR-labeled nanogels, blue: nuclei stained with Hoechst 33258). (For interpretation of the references to colour in this figure legend, the reader is referred to the web version of this article.)

with neither azide trimannose nor AF488 azide was observed. Thus, these UV–Vis spectrophotometry data confirm the successful azide trimannose conjugation to the DBCO nanogels (Fig. 3C).

To assess the conserved bioactivity of trimannose towards interacting with the MMR/CD206 receptor and trigger a receptor-mediated cellular uptake for nanogels, we next performed *in vitro* experiments on Chinese Hamster Ovary cells that were genetically modified to express the MMR/CD206 receptor (CHO^{MMR+}), while wild type CHO cells without the MMR/CD206 receptor (CHO^{MMR-}) served as controls. For this purpose, both cell lines were incubated with the trimannose- or AF488-modified DBCO nanogel samples or the control nanogels for 24 h at 37 °C and characterized by flow cytometry and fluorescence confocal microscopy analyses. Thereby, our *in vitro* tests confirmed an exclusively boosted cellular uptake of trimannose-conjugated DBCO nanogels by CHO^{MMR+} cells compared to CHO^{MMR-}, visualized by the histogram plot (Fig. 3D) and mean fluorescence intensities (Fig. 3E), both recorded by flow cytometry. Control nanogels without DBCO showed no cellular uptake in both cell lines (Figure S49-S51). Based on the increased hydrophobicity of the nanogel by conjugating the fluorescent dye AF488 to the DBCO group inside the nanogel core, the corresponding dye-labeled DBCO nanogels revealed an increased non-specific cellular uptake in both CHO^{MMR+} and CHO^{MMR-} cells compared to the highly selective trimannose-conjugated DBCO nanogels (Figure S49-S51). We assume that the high amount of multiple aromatic moieties (DBCO and AF488) drastically increases the hydrophobicity which results in non-specific protein and membrane interactions, as observed earlier [63]. Alternatively, the hydrophilic carbohydrate click modification prevents this and instead mediates receptor specific binding. Carbohydrates can consequently also serve as a sufficient shielding domain, as we could observe before, too [54,55]. Our findings were further supported by confocal microscopy images of CHO^{MMR+} and CHO^{MMR-} cells. All cells provided an internalization of AF488-labled DBCO nanogels, whereas trimannose-conjugation caused an exclusive cellular uptake in CHO^{MMR+} cells, confirming the successful targeting of the MMR/CD206 receptor by trimannose, followed by nanoparticle cell internalization (Fig. 3F and Figure S52-S53).

Altogether, the obtained results demonstrate the successful conjugation of trimannose-species in the core of the DBCO nanogels by click reaction without affecting their ability to selectively target the MMR receptor on CHO cells, leading to an enhanced specific cellular uptake.

2.3. Synthesis and characterization of an azide containing 2-Propionic-3-Methylmaleic anhydride linker for pH-Reversible amidation reaction

Based on these promising results, we wanted to verify whether the DBCO group inside the nanogel can also be explored for pH–sensitive covalent drug loading. Disubstituted maleic anhydride systems show a high sensitivity to slightly acidic environments, such as the tumor microenvironment (pH ≈ 6.5), able to release conjugated amines in their native form. Due to these features, maleic anhydrides are often referred to as traceless linkers [36,60]. We have recently reported on a polymer maleic anhydride system with remarkable drug delivery performances for immunostimulatory drugs, however, only when equipped with secondary amines [43]. To conjugate such a pH-sensitive linker into the core of our DBCO-functionalized nanogels, a disubstituted maleic anhydride needs to be equipped with an additional azide functionality for biorthogonal DBCO click reaction.

To this end, 2–propionic-3-methylmaleic anhydride was converted in a two-step reaction, starting with the transformation into a highly amine reactive acid chloride. Next, this reactive group was treated with the commercially available 11-azido-3,6–9-trioxaundecan-1-amine (Fig. 4A, Figure S22) affording a bifunctional linker that is both accessible for pH-reversible conjugation of secondary amines as well as azide click reaction to DBCO groups. With regard to this amidation reaction, we opted for the design of a stable amide bond as linker between the azide and the maleic anhydride than an ester bond. Thus, we circumvent premature ester hydrolysis that would compete with the acid-triggered drug release from the anhydride system. Finally, the resulted linker was characterized by ^{1}H and 2D NMR spectroscopy as well as IR spectroscopy measurement (Fig. 4B and Figure S23-S28).

After successful synthesis of the bifunctional linker, we evaluated its pH–reversible amine conjugation for fluorescent dyes in organic solvents. In this context, the azide-containing 2–propionic-3-methylmaleic anhydride linker was dissolved in DMSO supplemented with triethylamine (TEA) and treaded with the synthesized secondary amine dye 4-nitro-7-piperazino-2,1,3-benzoxadiazole (NBD-PZ/NBD, Figure S29-S31) or the commercially available primary amine dye dansyl cadaverine (Figure S32). Both fluorescent dyes demonstrated successful amidation of the anhydride system, although only the secondary amine containing NBD-PZ revealed an acidic release of the conjugated dye characterized by ^{1}H NMR spectroscopy measurements (Fig. 4C). Interestingly, secondary amines led to the formation of two asymmetric regioisomers and, consequently, the α–methyl signal of the *cis*-oriented double bond splits into two sharp signals (Fig. 4C, Signal e, neutral – and MALDI ToF MS measurements, Figure S33). Followed acidification with trifluoroacetic acid (TFA) forced the reformation of the disubstituted maleic anhydride structure by generation of one sharp α–methyl signal and the release of NBD-PZ (Fig. 4C, Signal e, acidic). Contrarily, the reaction with the primary amine dye dansyl cadaverine showed the formation of a pH–resistant imide structure, as confirmed both by ^{1}H NMR (affording one sharp α–methyl signal after amidation, Figure S34) as well as ESI-MS measurement (for the cyclized imide the molecular mass is reduced by 18 g/mol due to water elimination, Figure S35). These findings were again in agreement with our previous studies on polymeric maleic anhydrides also exhibiting an exclusive pH reversibility only upon reaction with secondary amines in DMSO [43]. Consequently, we focused our attention on the reversible conjugation of secondary amine–functionalized dyes and drugs during the following nanogel experiments.

For the preparation of pH-reversibly dye-labeled DBCO nanogels, NBD-PZ-modified azide–functionalized maleic anhydride linkers were introduced to the core-localized DBCO units or added to the control nanogels (Fig. 4D). To ensure the absence of unconjugated linkers, all samples were analogously purified by extensive spin-filtration (MWCO 10000 g/mol) with water supplemented with 0.1 % ammonia. Based on the previous fluorescent labeling of the azide-functionalized maleic anhydride linker, the nanogel dye modification could again be confirmed by UV–Vis spectroscopy, showing a further absorbance

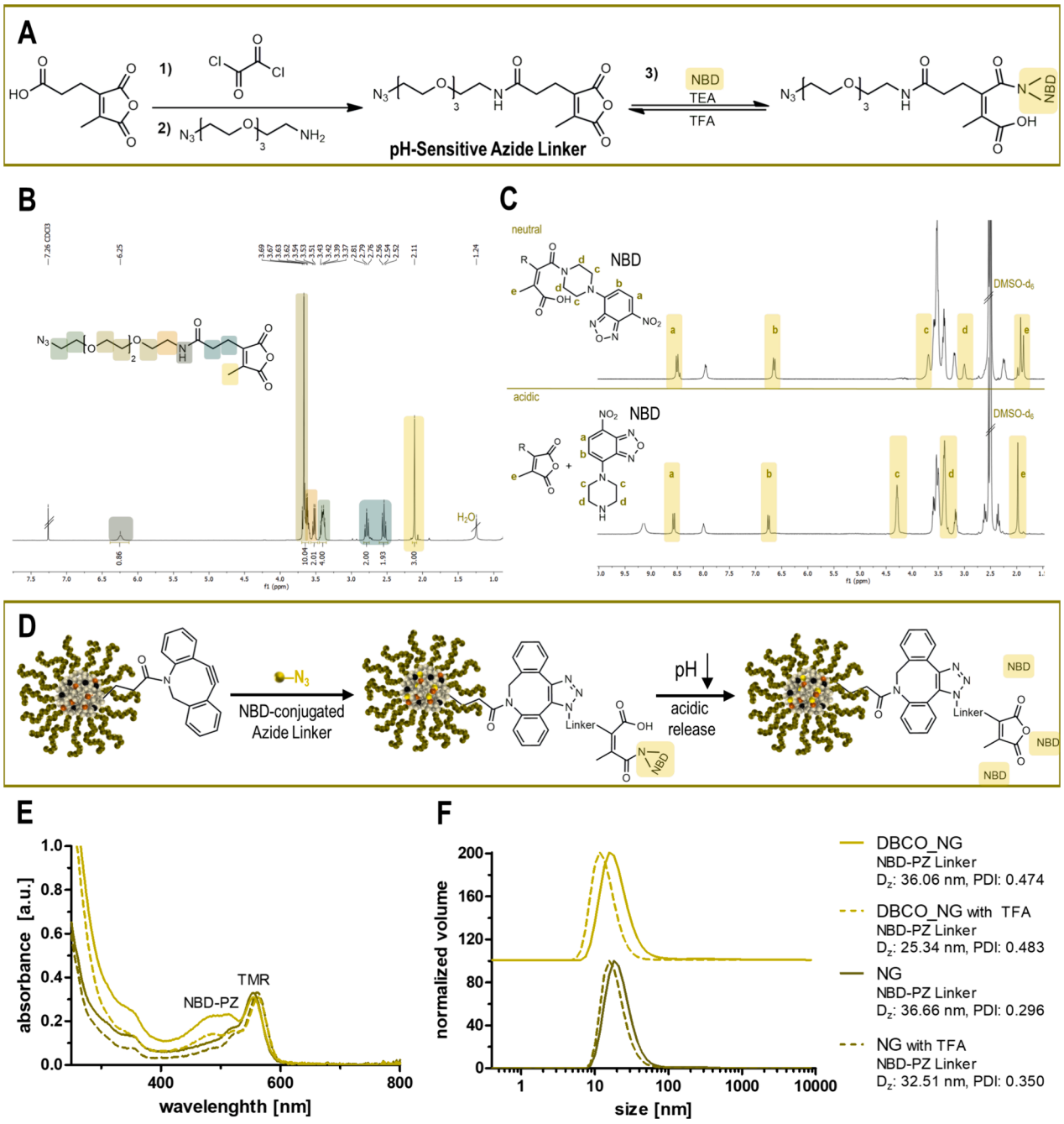

Fig. 4. Synthesis of a bifunctional linker, accessible for pH-reversible conjugation of secondary amines and azide click reaction to DBCO core-functionalized nanogels. (A) Synthesis route for the fabrication of a pH-sensitive linker based on 2-propionic-3-methylmaleic anhydride with additional azide functionality, followed by pH-reversible dye-labeling with the fluorescent dye NBD-PZ/NBD. (B) ^{1}H NMR spectrum of the pH-sensitive azide linker recorded in $CDCl_3$. (C) ^{1}H NMR spectra of the NBD–conjugated azide linker under neutral conditions and upon acidification showing the reversible conjugation and release of the fluorescent dye 4-nitro-7-piperazino-2,1,3-benzoxadiazole (NBD), in particular by the two asymmetric regioisomer signals of the α-methyl signal e that re-form again into one single sharp peak e upon acid-triggered anhydride formation. (D) Synthetic concept for the formation of pH-reversible NBD–labeled DBCO nanogels by reaction with the dye-conjugated azide linker. (E) UV–Vis spectroscopy measurements of the DBCO nanogel reacted with the NBD-labeled azide linker under neutral and acidic conditions (light green) compared to control nanogels treated with the dye-labeled linker (dark green). DBCO nanogels undergo a successful conjugation with the NBD-labeled linker (absorbance maximum at 480 nm) and release NBD after treatment with trifluoroacetic acid (TFA), while control nanogels remain unlabeled. (F) DLS measurement of the DBCO nanogels (light green) and control nanogels (dark green) that reacted with the dye-labeled linker as well as after treatment with TFA. (For interpretation of the references to colour in this figure legend, the reader is referred to the web version of this article.)

maximum at 480 nm only for the DCBO nanogels compared to the control nanogels (Fig. 4E). Additional treatment with TFA caused a successful release of conjugated NBD-PZ and removal during the following spin-filtration processes (Fig. 4E). All nanogels exhibited almost identical particle sizes after the treatment with the dye-labeled linker and slightly decreased by treatment with TFA (Fig. 4F). Thus, azide-containing 2–propionic-3-methylmaleic anhydride-based linkers represent ideal properties for pH–reversible conjugation of secondary amines and further modification of core-functionalized DBCO nanogels. Such pH-driven release scenarios may for instance become relevant with regards to intracellular endosomal drug delivery.

2.4. Formation of pH-releasable immunostimulatory DBCO nanogels

After having demonstrated efficient functionalization of DBCO nanogels with azide-clickable linkers which further provide additional pH-sensitive release properties for conjugated secondary amines, we used our bifunctional linker system for reversible covalent drug loading into our core-crosslinked nanoparticles. Potent small molecular activators of the Toll-like receptor 7 and 8 (TLR 7/8) demonstrate an attractive drug category for cancer immunotherapy. Already presented by us in several studies, conjugation of TLR 7/8 agonists promote their selective immune stimulation spatiotemporally while reducing unspecific side effects. Unfortunately, after conjugation to nano-sized carrier systems the immunodrug IMDQ often lacks its high nanomolar drug activity [22,44,47,48,61,62]. Therefore, we investigated the immune stimulatory profile of a pH-reversible IMDQ–loaded DBCO nanogel which would be able to release the conjugated drug under endolysosomal pH conditions by following the introduced bifunctional linker strategy (Fig. 5A).

First, the imidazoquinoline-based TLR 7/8 agonist IMDQ was modified in a two-step reaction, generating a secondary amine (IMDQ-Me, Figure S40-S43) for pH-reversible conjugation to the azide-clickable linker system (Figure S44 and S45). Next, the linker-drug conjugate could be attached to the DBCO nanogels and compared to control nanogels with no DBCO-groups and, thus, unable for click reactions (Fig. 5A). Prior to the first *in vitro* test, unbound linker-IMDQ-Me-conjugate was removed for all samples – in analogy to the previous experiments – by spin–filtration and the resulting drug load verified by UV–Vis spectroscopy. Thereby, only DBCO-functionalized nanogels revealed a successful conjugation with typical IMDQ-Me drug absorbances around 324 nm, corresponding to a drug loading of 3.1 wt% (Fig. 5B and Figure S48).

To finally investigate the IMDQ-Me-mediated TLR7/8 activity, RAW-Dual macrophages' reporter function was employed. Engineered RAW-Dual macrophages enable the screening of different TLR activities, for example, by evaluating the expression of embryonic alkaline phosphatase in response to NF–κB activation. Thereby, secreted embryonic alkaline phosphatase (SEAP) can easily be detected by UV–Vis spectroscopy of the cell culture supernatant after applying the Quanti Blue Assay. Consequently, RAW-Dual macrophages were incubated with increasing concentrations of the IMDQ-Me-linker-conjugated DBCO nanogel or soluble IMDQ–Me. Additionally, different control nanogels such as the empty nanogels (DBCO NG and NG) as well as nanogel (NG) treated with the linker-drug conjugate were analyzed. Remarkably, both the IMDQ-Me-loaded DBCO nanogel and soluble IMDQ-Me provided a strong TLR activation at the same sub-micromolar concentration range, while all empty controls induced no TLR stimulation and remained immunologically silent (Fig. 5D). The obtained results indicate for the first time similar TLR activation for a covalently bound agonist versus its soluble counterpart. This confirms successful acidic-triggered release of IMDQ-Me from the DBCO nanogel (presumably inside the endolysosomes) and, thus, explains its equal stimulatory effect to soluble IMDQ-Me. Additionally, RAW-Dual cell viability was quantified by a MTT Assay. Thereby, all tested samples demonstrated no significant toxicity in the studied concentration regime (Fig. 5C).

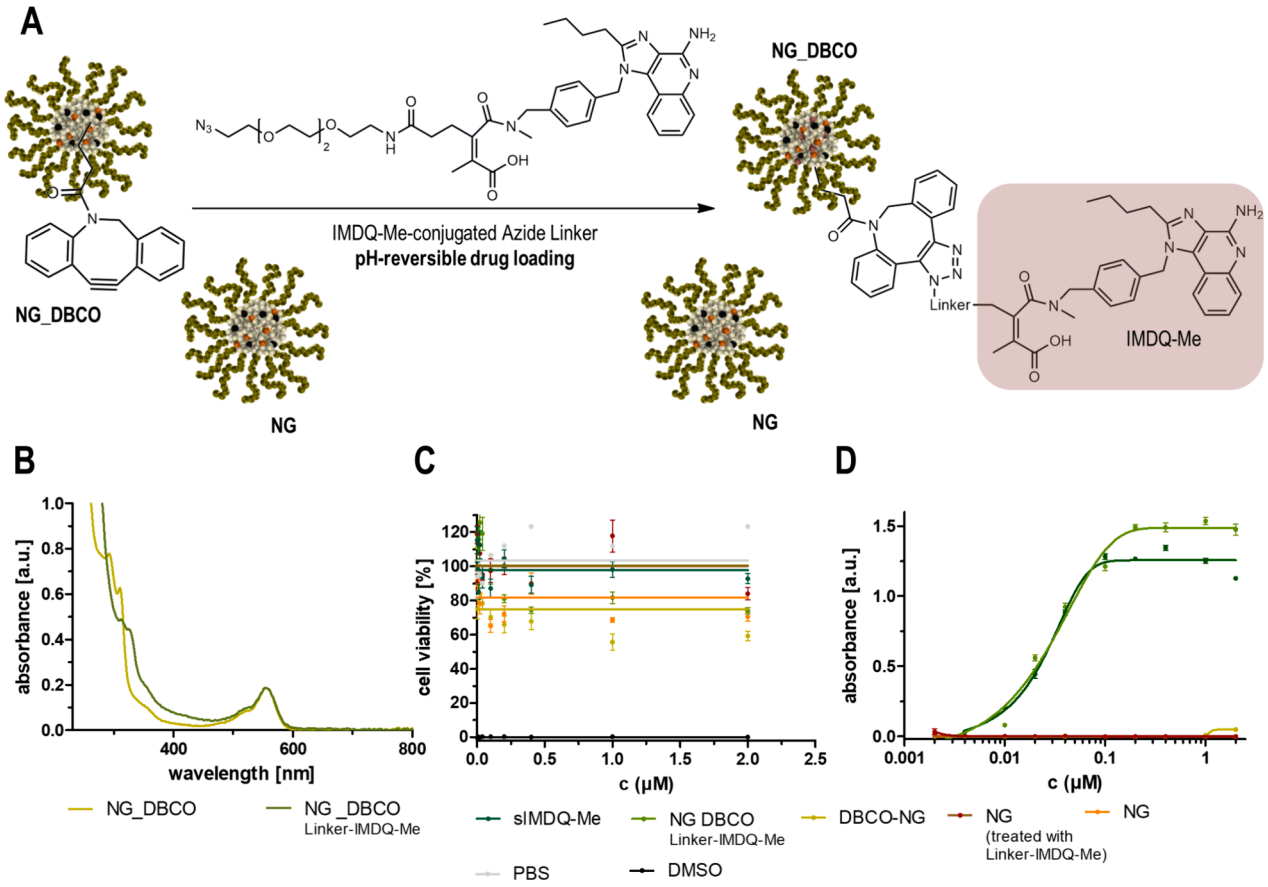

Fig. 5. *In vitro* evaluation of TMR-labeled DBCO nanogels with pH-reversibly attached immune stimulatory TLR 7/8 agonist IMDQ-Me. (A) Reaction strategy for the synthesis of immunodrug-loaded DBCO nanogels by treatment with IMDQ-Me-conjugated azide linker compared to nanogels without DBCO. (B) UV–Vis spectroscopy analysis of the fluorescently labeled DBCO nanogel before (dark green) and after pH–sensitive drug loading (light green). (C) Cell viability of RAW-Dual macrophages incubated with the drug-loaded DBCO nanogel, soluble IMDQ-Me, different control nanogels, as well as PBS and DMSO, quantified by MTT assay (n = 4). (D) TLR 7/8 receptor activation of soluble IMDQ-Me and the pH–reversibly IMDQ-Me-loaded DBCO nanogel compared to the empty DBCO nanogel and control nanogels determined by Quanti Blue assay (n = 4). (For interpretation of the references to colour in this figure legend, the reader is referred to the web version of this article.)

3. Conclusion

Overall, we have successfully demonstrated the RAFT-based synthesis and formulation of a core–functionalized DBCO nanogel platform serving as a chemically diverse toolbox for (reversible) bioorthogonal attachment of targeting units or small immunostimulatory molecules. In a subsequent controlled RAFT polymerization, reactive ester block copolymers were synthesized and partially DBCO modified. Based on the self-assembly properties in DMSO, precursor micelles could be generated, followed by amidation of the reactive ester side chains into core-crosslinked, hydrophilic nanogels. Besides the bioorthogonally well-addressable DBCO groups localized in the core, their sterical accessibility for click reactants corresponds well to the view of a more porous structure, as we could recently gain for similar micelle-derived core-crosslinked and hydrophilized nanogels [53]. In the current study, we could practice this with azide–functionalized dyes that could successfully be covalently incorporated into the nanogel cores. Moreover, the nanocarriers' potential for specific attachment of azide-containing bioactive groups was further demonstrated by the conjugation of a clickable trimannose as targeting unit for mannose-decorated immune cells, such as TAMs. First *in vitro* experiments demonstrated the selective delivery into MMR^+ CHO cells and, thus, encouraged the development of further pH-releasable drug delivery systems. By the synthesis of an azide–containing 2-propionic-3-methylmaleic anhydride-based linker we afforded a bifunctional linker with the ability for pH-reversible conjugation of secondary amines in polar aprotic solvents, such as DMSO, and further DBCO click reaction to the nanogels. Subsequently, secondary amine-modified IMDQ-Me, a highly potent TLR 7/8 agonist, was conjugated to the linker and then attached to the DBCO nanogels. Remarkably, the pH–sensitive drug-loading resulted in strong TLR 7/8 receptor stimulations *in vitro* that were of equal activity as the soluble drug itself. These finding underline the efficacy of the core–functionalized DBCO nanogels as a carrier platform for the specific targeting of immune cells and the pH-reversible endosomal delivery potential for small immune modulators. Given the opportunities of introducing also stimuli-responsive cross-links, [64–66] the development of DBCO-functionalized nanogels may pave the way for novel multifunctional carrier systems for therapeutic applications in cancer immunotherapy.

4. Associated content

The Supporting Information is available free of charge at: Details on the instruments, materials and methods, experimental protocols, and further characterization data are demonstrated in Figure S1-S53.

Author contributions

The manuscript was written through contribution of all authors. All authors have given approval to the final version of the manuscript.

CRediT authorship contribution statement

Alina G. Heck: Writing – review & editing, Writing – original draft, Visualization, Validation, Investigation. **David Schwiertz:** Methodology, Investigation. **Bellinda Lantzberg:** Methodology. **Ha-Chi Nguyen:** Methodology. **Robert Forster:** Methodology. **Maximilian Scherger:** Methodology. **Till Opatz:** Methodology. **Jo A. Van Ginderachter:** Methodology. **Lutz Nuhn:** Writing – review & editing, Writing – original draft, Supervision, Project administration, Methodology, Investigation, Funding acquisition, Formal analysis, Data curation, Conceptualization.

Declaration of competing interest

The authors declare that they have no known competing financial interests or personal relationships that could have appeared to influence the work reported in this paper.

Data availability

Data will be made available on request.

Acknowledgement

The authors' work was gratefully supported by the DFG through the Emmy Noether program and the CRC/SFB 1066 projects B03 and B04 (both to L.N.). Moreover, support by the BMBF Clusters4Futer curATime (projects curAIntervent and megATarget, both to L.N.) is kindly acknowledged. Manfred Wagner, Stefan Spang, Stephan Türk, Jutta Schnee and Detlev-Walter Scholdei are gratefully acknowledged for technical assistance during the analytical measurements. Moreover, we would like to thank Tanja Weil for providing access to excellent laboratory facilities.

Appendix A. Supplementary material

Supplementary data to this article can be found online at https://doi.org/10.1016/j.eurpolymj.2024.113150.

References

[1] H. Cabral, K. Miyata, K. Osada, K. Kataoka, Block copolymer micelles in nanomedicine applications, Chem. Rev. 118 (14) (2018) 6844–6892.
[2] S. Sur, A. Rathore, V. Dave, K.R. Reddy, R.S. Chouhan, V. Sadhu, Recent developments in functionalized polymer nanoparticles for efficient drug delivery system, Nano-Struct. Nano-Obj. 20 (2019) 100397.
[3] A. Kumari, S.K. Yadav, S.C. Yadav, Biodegradable polymeric nanoparticles based drug delivery systems, Colloids Surf. B Biointerf. 75 (1) (2010) 1–18.
[4] M. Talelli, M. Barz, C.J.F. Rijcken, F. Kiessling, W.E. Hennink, T. Lammers, Core-crosslinked polymeric micelles: principles, preparation, biomedical applications and clinical translation, Nano Today 10 (1) (2015) 93–117.
[5] Y. Shi, R. van der Meel, X. Chen, T. Lammers, The EPR effect and beyond: strategies to improve tumor targeting and cancer nanomedicine treatment efficacy, Theranostics 10 (17) (2020) 7921–7924.
[6] M.F. Attia, N. Anton, J. Wallyn, Z. Omran, T.F. Vandamme, An Overview of active and passive targeting strategies to improve the nanocarriers efficiency to tumour sites, J. Pharm. Pharmacol. 71 (8) (2019) 1185–1198.
[7] A.K. Pearce, R.K. O'Reilly, Insights into active targeting of nanoparticles in drug delivery: advances in clinical studies and design considerations for cancer nanomedicine, Bioconjug. Chem. 30 (9) (2019) 2300–2311.
[8] L. Gros, H. Ringsdorf, Polymeric antitumour agents on a molecular and on a cellular level? Polym. Sci. Technol. 23 (1983) 23–32.
[9] H. Ringsdorf, Structure and Properties of Pharmacologically Active Polymers, J. Polym. Sci. Polym. Symp. 153 (51) (1975) 135–153.
[10] M. Scherger, E. Bolli, A.R.P. Antunes, S. Arnouk, J. Stickdorn, A. Van Driessche, H. Schild, S. Grabbe, B.G. De Geest, J.A. Van Ginderachter, L. Nuhn, Transient multivalent nanobody targeting to CD206-expressing cells via PH-degradable nanogels, Cells 9 (10) (2020).
[11] E. Bolli, M. Scherger, S.M. Arnouk, A.R. Pombo Antunes, D. Straßburger, M. Urschbach, J. Stickdorn, K. De Vlaminck, K. Movahedi, H.J. Räder, S. Hernot, P. Besenius, J.A. Van Ginderachter, L. Nuhn, Targeted repolarization of tumor-associated macrophages via imidazoquinoline-linked nanobodies, Adv. Sci. 8 (10) (2021) 1–12.
[12] S. Kawakami, M. Hashida, Glycosylation-mediated targeting of carriers, J. Control. Release 190 (2014) 542–555.
[13] J.M. Irache, H.H. Salman, C. Gamazo, S. Espuelas, Mannose-targeted systems for the delivery of therapeutics, Expert Opin. Drug Deliv. 5 (6) (2008) 703–724.
[14] L. Nuhn, E. Bolli, S. Massa, I. Vandenberghe, K. Movahedi, B. Devreese, J.A. Van Ginderachter, B.G. De Geest, Targeting protumoral tumor-associated macrophages with nanobody-functionalized nanogels through strain promoted azide alkyne cycloaddition ligation, Bioconjug. Chem. 29 (7) (2018) 2394–2405.
[15] B. Ruffell, L.M. Coussens, Macrophages and therapeutic resistance in cancer, Cancer Cell 27 (4) (2015) 462–472.
[16] Z. Duan, Y. Luo, Targeting macrophages in cancer immunotherapy, Signal Transduct. Target. Ther. 6 (1) (2021) 1–21.
[17] A. Mantovani, F. Marchesi, A. Malesci, L. Laghi, P. Allavena, Tumor-associated macrophages as treatment targets in oncology, Nat Rev Clin Oncol 14 (7) (2017) 399–416.
[18] A. Blanazs, S.P. Armes, A.J. Ryan, Self-assembled block copolymer aggregates: from micelles to vesicles and their biological applications, Macromol. Rapid Commun. 30 (4–5) (2009) 267–277.
[19] J. Kockelmann, R. Zentel, L. Nuhn, Post-polymerization modifications to prepare biomedical nanocarriers with varying internal structures, their properties and impact on protein corona formation, Macromol. Chem. Phys. 2300199 (2023) 1–15.
[20] N. Leber, L. Nuhn, R. Zentel, Cationic nanohydrogel particles for therapeutic oligonucleotide delivery, Macromol. Biosci. 17 (10) (2017) 1–15.

[21] L. Nuhn, M. Hirsch, B. Krieg, K. Koynov, K. Fischer, M. Schmidt, M. Helm, R. Zentel, Cationic nanohydrogel particles as potential SiRNA carriers for cellular delivery, ACS Nano 6 (3) (2012) 2198–2214.
[22] J. Stickdorn, L. Nuhn, Reactive-ester derived polymer nanogels for cancer immunotherapy, Eur. Polym. J. 2020 (124) (September 2019) 109481.
[23] L. Nuhn, S. De Koker, S. Van Lint, Z. Zhong, J.P. Catani, F. Combes, K. Deswarte, Y. Li, B.N. Lambrecht, S. Lienenklaus, N.N. Sanders, S.A. David, J. Tavernier, B. G. De Geest, Nanoparticle-conjugate TLR7/8 agonist localized immunotherapy provokes safe antitumoral responses, Adv. Mater. 30 (45) (2018) 1–9.
[24] L. Nuhn, N. Vanparijs, A. De Beuckelaer, L. Lybaert, G. Verstraete, K. Deswarte, S. Lienenklaus, N.M. Shukla, A.C.D. Salyer, B.N. Lambrecht, J. Grooten, S.A. David, S. De Koker, B.G. De Geest, PH-Degradable Imidazoquinoline-Ligated Nanogels for Lymph Node-Focused Immune Activation, Proc. Natl. Acad. Sci. U. S. A. 113 (29) (2016) 8098–8103.
[25] J. Stickdorn, L. Stein, D. Arnold-Schild, J. Hahlbrock, C. Medina-Montano, J. Bartneck, T. Ziß, E. Montermann, C. Kappel, D. Hobernik, M. Haist, H. Yurugi, M. Raabe, A. Best, K. Rajalingam, M.P. Radsak, S.A. David, K. Koynov, M. Bros, S. Grabbe, H. Schild, L. Nuhn, Systemically administered TLR7/8 agonist and antigen-conjugated nanogels govern immune responses against tumors, ACS Nano 16 (3) (2022) 4426–4443.
[26] J. Stickdorn, C. Czysch, C. Medina-Montano, L. Stein, L. Xu, M. Scherger, H. Schild, S. Grabbe, L. Nuhn, Peptide-decorated degradable polycarbonate nanogels for eliciting antigen-specific immune responses, Int. J. Mol. Sci. 24 (20) (2023).
[27] D. Hein, C. Liu, X. Ming, D. Wang, Click Chemistry, a Powerful Tool for Pharmaceutical Sciences, Natl. Inst. Heal. J. 25 (10) (2008) 1–7.
[28] H.C. Kolb, M.G. Finn, K.B. Sharpless, Click chemistry: diverse chemical function from a few good reactions, Angew. Chemie - Int. Ed. 40 (11) (2001) 2004–2021.
[29] S.L. Scinto, D.A. Bilodeau, R. Hincapie, W. Lee, S.S. Nguyen, M. Xu, C.W. am Ende, M.G. Finn, K. Lang, Q. Lin, J.P. Pezacki, J.A. Prescher, M.S. Robillard, Fox, J. m. Bioorthogon. Chem. Nat. Rev. Methods Prim. 1 (1) (2021).
[30] R.E. Bird, S.A. Lemmel, X. Yu, Q.A. Zhou, Bioorthogonal chemistry and its applications, Bioconjug. Chem. 32 (12) (2021) 2457–2479.
[31] N.J. Agard, J.A. Prescher, C.R. Bertozzi, A strain-promoted [3 + 2] azide-alkyne cycloaddition for covalent modification of biomolecules in living systems, J. Am. Chem. Soc. 126 (46) (2004) 15046–15047.
[32] P. Schattling, F.D. Jochum, P. Theato, Multi-stimuli responsive polymers-the all-in-one talents, Polym. Chem. 5 (1) (2014) 25–36.
[33] R. Tong, L. Tang, L. Ma, C. Tu, R. Baumgartner, J. Cheng, Smart chemistry in polymeric nanomedicine, Chem. Soc. Rev. 43 (20) (2014) 6982–7012.
[34] E. Fleige, M.A. Quadir, R. Haag, Stimuli-responsive polymeric nanocarriers for the controlled transport of active compounds: concepts and applications, Adv. Drug Deliv. Rev. 64 (9) (2012) 866–884.
[35] A. Van Driessche, A. Kocere, H. Everaert, L. Nuhn, S. Van Herck, G. Griffiths, F. Fenaroli, B.G. De Geest, PH-sensitive hydrazone-linked doxorubicin nanogels via polymeric-activated ester scaffolds: synthesis, assembly, and in vitro and in vivo evaluation in tumor-bearing zebrafish, Chem. Mater. 30 (23) (2018) 8587–8596.
[36] J.Z. Du, H.J. Li, J. Wang, Tumor-acidity-cleavable maleic acid amide (TACMAA): a powerful tool for designing smart nanoparticles to overcome delivery barriers in cancer nanomedicine, Acc. Chem. Res. 51 (11) (2018) 2848–2856.
[37] M. Kanamala, W.R. Wilson, M. Yang, B.D. Palmer, Z. Wu, Mechanisms and biomaterials in PH-responsive tumour targeted drug delivery: a review, Biomaterials 85 (2016) 152–167.
[38] M.V. Spanedda, L. Bourel-Bonnet, Cyclic anhydrides as powerful tools for bioconjugation and smart delivery, Bioconjug. Chem. 32 (3) (2021) 482–496.
[39] X. Zhang, K. Zhang, R. Haag, Multi-stage, charge conversional, stimuli-responsive nanogels for therapeutic protein delivery, Biomater. Sci. 3 (11) (2015) 1487–1496.
[40] A. Zhang, L. Yao, M. An, Reversing the undesirable PH-profile of doxorubicin: via activation of a di-substituted maleamic acid prodrug at tumor acidity, Chem. Commun. 53 (95) (2017) 12826–12829.
[41] S. Su, F.S. Du, Z.C. Li, Synthesis and PH-dependent hydrolysis profiles of mono- and dialkyl substituted maleamic acids, Org. Biomol. Chem. 15 (39) (2017) 8384–8392.
[42] Y. Song, D. Jung, S. Kang, Y. Lee, Amine-selective affinity resins based on PH-sensitive reversible formation of covalent bonds, Soft Matter 13 (12) (2017) 2295–2298.
[43] A.G. Heck, J. Stickdorn, L.J. Rosenberger, M. Scherger, J. Woller, K. Eigen, M. Bros, S. Grabbe, L. Nuhn, Polymerizable 2-propionic-3-methylmaleic anhydrides as a macromolecular carrier platform for PH-responsive immunodrug delivery, J. Am. Chem. Soc. 145 (50) (2023) 27424–27436.
[44] S. Van Herck, B.G. De Geest, Nanomedicine-mediated alteration of the pharmacokinetic profile of small molecule cancer immunotherapeutics, Acta Pharmacol. Sin. 41 (7) (2020) 881–894.
[45] L. Lybaert, K. Vermaelen, B.G. De Geest, L. Nuhn, Immunoengineering through cancer vaccines – a personalized and multi-step vaccine approach towards precise cancer immunity, J. Control. Release 289 (2018) 125–145.
[46] J. Kockelmann, J. Stickdorn, S. Kasmi, J. De Vrieze, M. Pieszka, D.Y.W. Ng, S. A. David, B.G. De Geest, L. Nuhn, Control over imidazoquinoline immune stimulation by PH-degradable poly(norbornene) nanogels, Biomacromolecules 21 (6) (2020) 2246–2257.
[47] C. Czysch, C. Medina-Montano, Z. Zhong, A. Fuchs, J. Stickdorn, P. Winterwerber, S. Schmitt, K. Deswarte, M. Raabe, M. Scherger, F. Combes, J. De Vrieze, S. Kasmi, N.N. Sandners, S. Lienenklaus, K. Koynov, H.J. Räder, B.N. Lambrecht, S.A. David, M. Bros, H. Schild, S. Grabbe, B.G. De Geest, L. Nuhn, Transient lymph node immune activation by hydrolysable polycarbonate nanogels, Adv. Funct. Mater. 32 (35) (2022) 2203490.
[48] A. Huppertsberg, L. Kaps, Z. Zhong, S. Schmitt, J. Stickdorn, K. Deswarte, F. Combes, C. Czysch, J. De Vrieze, S. Kasmi, N. Choteschovsky, A. Klefenz, C. Medina-Montano, P. Winterwerber, C. Chen, M. Bros, S. Lienenklaus, N. N. Sanders, K. Koynov, D. Schuppan, B.N. Lambrecht, S.A. David, B.G. De Geest, L. Nuhn, Squaric ester-based, PH-degradable nanogels: modular nanocarriers for safe, systemic administration of toll-like receptor 7/8 agonistic immune modulators, J. Am. Chem. Soc. 143 (26) (2021) 9872–9883.
[49] M. Eberhardt, R. Mruk, R. Zentel, P. Théato, Synthesis of pentafluorophenyl(meth) acrylate polymers: new precursor polymers for the synthesis of multifunctional materials, Eur. Polym. J. 41 (7) (2005) 1569–1575.
[50] M.I. Gibson, E. Froehlich, H.-A. Klok, Postpolymerization modification of poly (pentafluorophenylmethacrylate): synthesis of a divers water-soluble polymer library, J. Polym. Sci. Part A Polym. Chem. 47 (2009) 4332–4345.
[51] N. Mohr, M. Barz, R. Forst, R. Zentel, A deeper insight into the postpolymerization modification of polypenta fluorophenyl methacrylates to poly(N-(2-hydroxypropyl) methacrylamide), Macromol. Rapid Commun. 35 (17) (2014) 1522–1527.
[52] A. Das, P. Theato, Activated ester containing polymers: opportunities and challenges for the design of functional macromolecules, Chem. Rev. 116 (3) (2016) 1434–1495.
[53] A. Huppertsberg, C. Leps, I. Alberg, C. Rosenauer, S. Morsbach, K. Landfester, S. Tenzer, R. Zentel, L. Nuhn, Squaric ester-based nanogels induce no distinct protein corona but entrap plasma proteins into their porous hydrogel network, Macromol. Rapid Commun. 43 (19) (2022) 1–9.
[54] N. Leber, L. Kaps, A. Yang, M. Aslam, M. Giardino, A. Klefenz, N. Choteschovsky, S. Rosigkeit, A. Mostafa, L. Nuhn, D. Schuppan, R. Zentel, α-mannosyl-functionalized cationic nanohydrogel particles for targeted gene knockdown in immunosuppressive macrophages, Macromol. Biosci. 19 (7) (2019) 1–12.
[55] L. Kaps, N. Leber, A. Klefenz, N. Choteschovsky, R. Zentel, L. Nuhn, D. Schuppan, In vivo SiRNA delivery to immunosuppressive liver macrophages by α-mannosyl-functionalized cationic nanohydrogel particles, Cells 9 (8) (2020).
[56] R. De Coen, N. Vanparijs, M.D.P. Risseeuw, L. Lybaert, B. Louage, S. De Koker, V. Kumar, J. Grooten, L. Taylor, N. Ayres, S. Van Calenbergh, L. Nuhn, B.G. De Geest, PH-degradable mannosylated nanogels for dendritic cell targeting, Biomacromolecules 17 (7) (2016) 2479–2488.
[57] R. De Coen, L. Nuhn, B.G. De Geest, Engineering mannosylated nanogels with membrane-disrupting properties, Polym. Chem. 10 (31) (2019) 4297–4304.
[58] K. Wagener, M. Bros, M. Krumb, J. Langhanki, S. Pektor, M. Worm, M. Schinnerer, E. Montermann, M. Miederer, H. Frey, T. Opatz, F. Rösch, Targeting of immune cells with trimannosylated liposomes, Adv. Ther. 3 (6) (2020) 1–10.
[59] M. Krumb, M.L. Frey, J. Langhanki, R. Forster, D. Kowalczyk, V. Mailänder, K. Landfester, T. Opatz, Multivalency beats complexity: a study on the cell uptake of carbohydrate functionalized nanocarriers to dendritic cells, Cells 9 (9) (2020).
[60] K. Maier, E. Wagner, Acid-labile traceless click linker for protein transduction, J. Am. Chem. Soc. 134 (24) (2012) 10169–10173.
[61] G.M. Lynn, R. Laga, C.M. Jewell, Induction of anti-cancer T cell immunity by in situ vaccination using systemically administered nanomedicines, Cancer Lett. 459 (January) (2019) 192–203.
[62] C.W. Shields, L.L.W. Wang, M.A. Evans, S. Mitragotri, Materials for immunotherapy, Adv. Mater. 32 (13) (2020) 1–56.
[63] M. Scherger, Y.A. Pilger, J. Stickdorn, P. Komforth, S. Schmitt, K. Koynov, H. J. Räder, L. Nuhn, Efficient self-immolative RAFT end group modification for macromolecular immunodrug delivery, Biomacromolecules 24 (5) (2023) 2380.
[64] L. Nuhn, L. Braun, I. Overhoff, A. Kelsch, D. Schaeffel, K. Koynov, R. Zentel, Degradable cationic nanohydrogel particles for stimuli-responsive release of siRNA, Macromol. Rapid. Commun. 35 (24) (2014) 2057–2064.
[65] N. Leber, L. Kaps, M. Aslam, J. Schupp, A. Brose, D. Schaeffel, K. Fischer, M. Diken, D. Strand, K. Koynov, A. Tuettenberg, L. Nuhn, R. Zentel, D. Schuppan, SiRNA-mediated in vivo gene knockdown by acid-degradable cationic nanohydrogel particles, J. Controlled Release 248 (2017) 10–23.
[66] L. Nuhn, S. Van Herck, A. Best, K. Deswarte, M. Kokkinopoulou, I. Lieberwirth, K. Koynov, B.N. Lambrecht, B.G. De Geest, FRET monitoring of intracellular ketal hydrolysis in synthetic nanoparticles, Angew. Chem. Int. Ed. 57 (33) (2018) 10760–10764.